OPTICAL TOMOGRAPHY FOR SOLID GAS MEASUREMENT USING MIXED PROJECTION

SITI ZARINA MOHD MUJI

A thesis submitted in fulfilment of the
requirements for the award of the degree of
Doctor of Philosophy (Electrical Engineering)

Faculty of Electrical Engineering
Universiti Teknologi Malaysia

JUNE 2012

ABSTRACT

Optical tomography is widely known in tomography area to visualise and measure mass flow rate of two phases flows solid gas. In order to visualise the material inside the pipeline, parallel beam projection had been selected at all times because of its simplicity. However while producing the image, some constraints such as smear and blurriness will happen, whereas for mass flow rate, the measurement of a non-homogenous flow will always affect the accuracy of the result. Therefore, a combination between parallel and fan beam was done to produce a better spatial resolution. This research introduces a new projection technique by mixing the parallel and fan beam projections that is, Mix Modality between Parallel and Fan Beam Left and Right (MPFBLR), and Mix Modality between Parallel and Fan Beam Centre (MPFBC). These mixed projections need a specific design of a sensor jig by eliminate the collimator to enable two modes of projections to be operated and consequently, this combination will use switching/pulsing technique. Linear Back Projection (LBP) is the algorithm that will be used to reconstruct the image in real time. The image will be processed offline to filter unwanted data, and to enhance quality using Filtered Back Projection (FBP) with Averaging Grouping Color (AGC) method and Linear Back Projection with Interpolation (LBPI). A new technique using polynomial graph acquired from calibration process of gravity flow rig will be employed to measure the mass flow rate. The result demonstrated that MPFBLR gave the best values in terms of Area Error (AE) percentage, Peak Signal to Noise Ratio (PSNR) and Normalized Mean Square Error (NMSE) compared to single parallel beam projection. The mass flow rate can be easily monitored using polynomial equation from the manual calibration. In conclusion, the combination technique between parallel and fan beam can improve the image quality and enable the mass flow rate measurement.

ABSTRAK

Tomografi optik diketahui secara meluas dalam bidang tomografi untuk menggambarkan dan mengukur kadar aliran jisim dalam dua aliran fasa pepejal gas. Untuk melihat bahan di dalam saluran paip, pancaran selari sentiasa dipilih kerana ia ringkas. Namun semasa imej dihasilkan, beberapa kekangan seperti imej yang samar dan kabur akan terjadi, manakala bagi kadar aliran jisim, pengukuran aliran tak homogen selalu memberi kesan kepada kejituan keputusan. Oleh itu, gabungan antara selari dan mencapah telah dilakukan untuk menghasilkan resolusi ruang yang lebih baik. Kajian ini memperkenalkan teknik pancaran yang baru dengan menggabungkan pancaran selari dan mencapah iaitu Campuran Modaliti antara Selari dan Mencapah Kiri dan Kanan (MPFBLR), dan Campuran Modaliti antara Selari dan Mencapah di Tengah (MPFBC). Campuran pancaran ini memerlukan rekabentuk khusus untuk jig penderia dengan membuang pemfokus cahaya bagi membolehkan dua mod pancaran beroperasi dan seterusnya kombinasi ini akan menggunakan teknik pensuisan/denyutan. Pancaran Kembali Linear (LBP) adalah algoritma yang akan digunakan untuk membina semula imej dalam masa nyata. Imej akan diproses secara luar talian untuk menapis sebarang data yang tidak dikehendaki dan menambahkan kualiti menggunakan Pancaran Kembali di Tapis (FBP) dengan teknik Pengumpulan Pemurataan Warna (AGC) dan Pancaran Kembali Linear dengan Penentudalaman (LBPI). Satu teknik baru yang menggunakan graf “polynomial” yang diperolehi dari proses penentukuran paip aliran graviti akan digunakan untuk mengukur kadar aliran jisim. Hasilnya menujukkan MPFBLR memberikan hasil yang terbaik dari segi peratusan Ralat Kawasan (AE), Puncak Isyarat kepada Nisbah Hingar (PSNR) dan Min Ternormal Ralat Kuasa Dua (NMSE) berbanding pancaran selari tunggal. Kadar aliran jisim adalah mudah dipantau menggunakan persamaan “polynomial” dari penentukuran insani. Kesimpulannya teknik gabungan selari dan mencapah boleh meningkatkan kualiti imej dan membolehkan pengukuran kadar aliran jisim.

TABLE OF CONTENTS

CHAPTER	TITLE	PAGE
	DECLARATION	**ii**
	DEDICATION	**iii**
	ACKNOWLEDGEMENTS	**iv**
	ABSTRACT	**v**
	ABSTRAK	**vi**
	TABLE OF CONTENTS	**vii**
	LIST OF TABLES	**xii**
	LIST OF FIGURES	**xv**
	LIST OF ABBREVIATIONS	**xxi**
	LIST OF SYMBOLS	**xxiii**
	LIST OF APPENDICES	**xxv**
1	**INTRODUCTION**	**1**
	1.1 Background Research Problem	3
	1.2 Problem Statements	4
	1.3 Aim and Objectives of the Study	5
	1.3.1 Aim	5
	1.3.2 Specific Objectives	5
	1.4 Scopes of the Study	6
	1.5 Significant Research Contribution	6
	1.6 Organization of the Thesis	7

2 LITERATURE REVIEW 9

2.1 Introduction 9

2.2 Introduction to Process Tomography 10

2.3 Types of Tomography Sensors 11

2.3.1 Electrical Capacitance Tomography (ECT) 11

2.3.2 Electrical Impedance Tomography (EIT) 11

2.3.3 Ultrasonic Tomography 12

2.3.4 Positron Emission Tomography (PET) 13

2.3.5 X-Ray Tomography 13

2.3.6 Optical Tomography 14

2.4 Recent research in Optical Tomography 15

2.5 Overview of Transmitter and Receiver used in Optical Tomography 16

2.5.1 Transmitter 16

2.5.2 Receiver 17

2.6 The Selection of Optical Sensor and Projection Arrangement: Advantages and Disadvantages 18

2.6.1 Fiber Optic and Parallel Mode 19

2.6.2 LED and Fan Beam Mode 21

2.6.3 Infrared Led and Parallel Beam Mode 22

2.6.4 Infrared Led and Fan Beam Mode 27

2.6.5 Laser and Parallel Beam Mode 29

2.6.6 Laser and Fan Beam Mode 29

2.6.7 Dual Mode Tomography 31

2.6.8 Summary of Sensor and Projection Types 32

2.7 Image Reconstruction Algorithm 32

2.7.1 Linear Back Projection Algorithm 33

2.7.2 Other Algorithms 37

2.7.3 Summary of Image Reconstruction Algorithm 38

2.8 Mass Flow Rate Measurement 38

2.9 Summary 40

3 OPTICAL TOMOGRAPHY MODELLING 41

3.1 Introduction 41

3.2 Optical Attenuation Model 41
3.3 Linear Model for Optical Tomography 44
3.4 Modelling the projection effect 47
3.4.1 Parallel Beam Projection 48
3.4.1.1 Orthogonal Projection 50
3.4.1.2 Rectilinear Projection 57
3.4.2 Fan Beam Projection 64
3.4.2.1 Fan Beam Centre (FBC) 67
3.4.2.2 Fan Beam Left and Right (FBLR) 68
3.4.3 Combination Technique 70
3.4.3.1 Modeling of Mix Modality between Parallel and Fan Beam Centre (MPFBC) 70
3.4.3.2 Modeling of Mix Modality between Parallel and Fan Beam Left and Right (MPFBLR) 71
3.5 Measurement Parameter 72
3.5.1 Concentration Profile 72
3.5.2 Mass Flow Rate measurement 74
3.5.3 Calibration Result of Mass Flow Rate Measurement 79
3.6 Summary 82

4 IMAGE RECONSTRUCTION 83
4.1 Introduction 83
4.2 Image Reconstruction Algorithms 84
4.3 Linear Back Projection (LBP) 85
4.3.1 Linear Back Projection (LBP): PB Projection 85
4.3.2 Linear Back Projection (LBP): FBC Projection 86
4.3.3 Linear Back Projection (LBP): FBLR projection 87
4.3.4 Linear Back Projection (LBP): MPFBC projection 89
4.3.5 Linear Back Projection (LBP): MPFBLR projection 91
4.4 Interpolation technique : Linear Back Projection with Interpolation (LBPI) 93
4.5 Filtered Back Projection (FBP) 93

4.6 Parameter for Image Analysis 98
4.7 Modeling Result 99
4.7.1 Single Model 100
4.7.1.1 Result for SPFM16 Model 101
4.7.1.2 Result for SPFM32 Model 103
4.7.1.3 Result for FFM Model 104
4.7.1.4 Single Model Analysis 105
4.7.2 Multiple Model 111
4.7.2.1 Result for Multiple Model 112
4.7.2.2 Multiple Model Analysis 117
4.8 Summary 125

5 HARDWARE AND SOFTWARE DEVELOPMENT 126
5.1 Introduction 126
5.2 Hardware Development 127
5.2.1 Sensor Selection 128
5.2.1.1 Photodiode Selection 129
5.2.1.2 Transmitter Sensor Selection 131
5.2.2 Optical Circuit 132
5.2.2.1 Optical Transmitter 132
5.2.2.2 Optical Receiver (Signal Conditioning Unit) 133
5.2.3 Controller Unit 137
5.2.4 Data Acquisition 138
5.2.5 PCB Circuit 142
5.3 Software Development 145
5.4 Summary 159

6 EXPERIMENT, RESULT AND ANALYSIS 160
6.1 Introduction 160
6.2 Experiment Procedure 161
6.2.1 Sensor Linearity and System Repeatability 161

6.2.2 Static Experiment 162
6.2.3 Dynamic Experiment 165
6.3 Result: Sensor Linearity and Repeatability 168
6.4 Result: Static Experiment 170
6.4.1 Static Experiment for Single Object 170
6.4.2 Analysis for single object 178
6.4.3 Comparison between Modeling and Experiment for Single Object 181
6.4.4 Static Experiment for Multiple Object 184
6.4.5 Analysis for Multiple Objects 195
6.4.6 Comparison between Modeling and Experiment for Multiple Object 200
6.5 Result: Dynamic Experiment 206
6.5.1 Concentration Profile Measurement 206
6.5.1.1 Baffle at the Bottom 206
6.5.1.2 Baffle at the Centre (MPFBLR) 208
6.5.1.3 Baffle at the Top (MPFBLR) 210
6.5.2 Mass Flow Rate Experiment 210
6.6 Summary 214

7 CONCLUSIONS AND FUTURE WORKS 215
7.1 Conclusions 215
7.2 Contribution 216
7.3 Recommendation for Future Works 217

REFERENCES 219
Appendices A – F 229-274

LIST OF TABLES

TABLE NO.	TITLE	PAGE
3.1	Predicted voltage drop and voltage loss for each obstacle diameter	46
3.2	The millimetre unit convert to pixel unit	53
3.3	Millimeter conversion to pixel for $r/2$, parameter.	60
3.4	The calculation of percentage of opening area in the baffle	78
3.5	Mass flow rate measurement	80
4.1	Single Flow Model and its characteristics	101
4.2	Simulation of three projection techniques towards SPFM16 flow model using LBP and FBP	102
4.3	Simulation of all projection techniques towards SPFM32 flow model using LBP and FBP algorithm	103
4.4	Simulation of all projection techniques towards FFM flow model using LBP algorithm	105
4.5	The Area Error Teory (AE_T %) for single flow model using FBP algorithm via simulation mode	105
4.6	PSNR and NMSE value for single flow model using LBP algorithm via simulation mode	106
4.7	PSNR and NMSE value for single flow model using FBP algorithm via simulation mode	108
4.8	Five flow model for multiple object and its characteristic	111
4.9	Simulation of all projection techniques towards Flow A model using LBP and FBP algorithm	112
4.10	Simulation of all projection techniques towards Flow B model using LBP and FBP algorithm	114
4.11	Simulation of all projection techniques towards Flow C	

	model using LBP and FBP algorithm	115
4.12	Simulation of all projection techniques towards Flow D model using LBP and FBP algorithm	116
4.13	Simulation of all projection techniques towards Flow E model using LBP and FBP algorithm	117
4.14	The AE_T percentage for various types of multiple flow models using FBP algorithm	118
4.15	PSNR and NMSE value for multiple flow models using LBP algorithm via simulation mode	119
4.16	PSNR and NMSE value for multiple flow model using FBP algorithm via simulation mode	121
5.1	The advantages and disadvantages between photodiode and phototransistor	129
5.2	The receivers' number and its corresponding saving location for side A and E	142
5.3	The number of storage in a buffer	142
6.1	Single and multiple objects in static experiment	163
6.2	Repeatability testing over 20 samples for all type of projection	169
6.3	SPFM16 model in 2D and 3D tomogram image for PB, MPFBC and MPFBLR projections using LBP algorithm	171
6.4	Post Processing Technique towards PB, MPFBC and MPFBLR projection using LBPI and FBP using AGC method for SPFM16 Model	173
6.5	SPFM32 model in 2D and 3D tomogram image for PB, MPFBC and MPFBLR projections using LBP algorithm	174
6.6	Post Processing Technique towards PB, MPFBC and MPFBLR projection using Interpolation and Filtering Process for SPFM32 Model	176
6.7	FFM model in 2D and 3D tomogram image for PB, MPFBC and MPFBLR projections using LBP algorithm	177
6.8	The Area Error Experiment (AE_E) for FFM Model via experiment mode	178
6.9	The Area Error Experiment (AE_E) for single flow model	

	using FBP algorithm via experimental works	179
6.10	Model A in 2D and 3D tomogram image for PB, MPFBC and MPFBLR projections using LBP algorithm	185
6.11	Post processing technique towards PB, MPFBC and MPFBLR projection using LBPI and FBP Process for Model A	186
6.12	Model B in 2D and 3D tomogram image for PB, MPFBC and MPFBLR projections using LBP algorithm	187
6.13	Post processing technique towards PB, MPFBC and MPFBLR projection using LBPI and FBP Process for Model B.	188
6.14	Model C in 2D and 3D tomogram image for PB, MPFBC and MPFBLR projections using LBP algorithm	189
6.15	Post processing technique towards PB, MPFBC and MPFBLR projection using LBPI and FBP Process for Model C	191
6.16	Model D in 2D and 3D tomogram image for PB, MPFBC and MPFBLR projections using LBP algorithm	192
6.17	Post processing technique towards PB, MPFBC and MPFBLR projection using LBPI and FBP Process for Model D	193
6.18	Model E in 2D and 3D tomogram image for PB, MPFBC and MPFBLR projections using LBP algorithm	194
6.19	Post processing technique towards PB, MPFBC and MPFBLR projection using LBPI and FBP process for Model E	195
6.20	The Area Error Experiment (AEE) percentage for various types of multiple flow models using FBP algorithm via experimental work	196
6.21	Implementing FBP using AGC type 5 in the filtering technique	204
6.22	Comparison between parallel, fan beam and mix projection	207
6.23	Baffle at the centre	208
6.24	Baffle at the Top (MPFBLR)	210
6.25	Concentration profile for different baffle opening	211
6.26	The difference between measured and calibration mass flow rate	212

LIST OF FIGURES

FIGURE NO.	TITLE	PAGE
2.1	Optical tomography system	10
2.2	a) Parallel beam projection, b) fan beam projection	18
2.3	Sensor arrangement used 16 pairs of sensor	22
2.4	Two layer of projection by Pang, (2004)	24
2.5	One layer of sensor jig by Goh (2005)	26
2.6	Sensor arrangement using 32 pairs of sensor	28
2.7	LBP algorithm	34
2.8	Image of (a) pure GBP and (b)FBPF +HRA	37
3.1	The sensor jig development a) Overall view b) Sensor jig model c) Acrylic pipe separation	43
3.2	Maximum Voltage, $Vmax$ for the receiver	44
3.3	An object in diameter of $'d'$mm is situated between transmitter and receiver result in voltage drop,$Vdrop$	44
3.4	1 mm obstacle is placed between transmitter and receiver	45
3.5	Linear relation between voltage losses against object diameter using numerical method	47
3.6	All projections of parallel beam ; orthogonal and rectilinear projections	49
3.7	The line of light for first orthogonal projection that is referred to Tx0 until Tx19	50
3.8	The line of light for second orthogonal projection that is referred to Tx 20 until Tx39	51
3.9	The dimension configuration for transducer in the sensor jig in millimeter unit	52

3.10	64x64 resolutions	54
3.11	The area calculation to create the sensitivity maps	55
3.12	A part of sensitivity maps from one view for Tx0 and Rx0	55
3.13	Sensitivity maps for first orthogonal projection	57
3.14	The coordinate for developing the sensitivity maps in rectilinear projection	58
3.15	The first view (Tx60-Rx60) and the last view (Tx79-Rx79) of sensitivity maps in the first rectilinear projection	60
3.16	The first view (Tx40-Rx40) and the last view (Tx59-Rx59) of sensitivity maps in the second rectilinear projection	63
3.17	Finding the fan beam coordinate using Microsoft Visio	66
3.18	Single projection for Fan Beam Centre Projection (FBC)	67
3.19	Fan Beam Centre Projection (FBC)	68
3.20	Single projection of FBLR type	69
3.21	Complete projection of Fan Beam Left and Right (FBLR)	69
3.22	Complete projection for MPFBC	71
3.23	Complete projection of MPFBLR	72
3.24	The gravity flow rig system	75
3.25	Calibration graph for mass flow rate versus flow indicator	76
3.26	Baffle sample as a concentration percentage indicator	77
3.27	The mass flow rate value using different baffle for 40 Hz flow indicator	81
4.1	Flow chart for FBP using AGC Bar until Type 5	97
4.2	AE_T (%) value for three types of single model using FBP algorithm via simulation mode	106
4.3	PSNR for different single flow model using LBP via simulation mode	107
4.4	NMSE for different single flow model using LBP via simulation mode.	107
4.5	PSNR for different single flow model using FBP via simulation mode	108
4.6	NMSE for different single flow model using FBP algorithm via simulation mode	109

4.7	The comparison of PSNR value between LBP and FBP algorithm in different single flow model and projection	109
4.8	The comparison of NMSE value between LBP and FBP algorithm in different single flow model and projection	110
4.9	AE_T (%) value for different multiple flow model using FBP algorithm via simulation mode	118
4.10	PSNR for different multiple flow model using LBP algorithm via simulation mode	119
4.11	NMSE for different multiple flow model using LBP algorithm via simulation mode	120
4.12	PSNR for different multiple flow model using FBP algorithm via simulation mode	121
4.13	NMSE for different multiple flow model using FBP algorithm via simulation mode	122
4.14	Comparison PSNR value between LBP and FBP algorithms for PB projection in different multiple flow model	122
4.15	The comparison of PSNR value between LBP and FBP algorithms for MPFBC projection in different multiple flow model	123
4.16	The comparison of PSNR value between LBP and FBP algorithms for MPFBLR projection in different multiple flow model	123
4.17	The comparison of NMSE value between LBP and FBP algorithms for PB projection in different multiple flow model	124
4.18	The comparison of NMSE value between LBP and FBP algorithms for MPFBC projection in different multiple flow model	124
4.19	The comparison of NMSE value between LBP and FBP algorithm for MPFBLR projection in different multiple flow model	125
5.1	Overall Optical Tomography System	128
5.2	The spectral range of sensitivity of SFH229FA	130
5.3	The spectral range of sensitivity of TSUS4300	131
5.4	Transmitter circuit	133

5.5	Receiver circuit	136
5.6	Receiver shows steady state mode after 34µs get the pulse from transmitter	136
5.7	Controller unit for slave operation	137
5.8	Interaction between slave and master in the data acquisition process	138
5.9	Circuit connection between master and slave	139
5.10	Flow chart for interaction between master and slave operation	139
5.11	The basic connection between slave and master	140
5.12	Sensor numbering in optical tomography	141
5.13	PCB Circuit (a) receiver circuit (b) transmitter circuit with controller (slave)	143
5.14	PCB for master circuit	144
5.15	The overall system	144
5.16	Application program graphic user interface (GUI) for online mode	145
5.17	Application program graphic user interface (GUI) for offline mode	146
5.18	Flow chart for online application programming	147
5.19	LBP algorithm for PB projection	148
5.20	LBP algorithm for FBC projection	149
5.21	LBP algorithm for FBLR projection	150
5.22	LBP algorithm for MPFBC projection	151
5.23	LBP algorithm for MPFBLR projection	151
5.24	Flow chart for offline application programming	152
5.25	LBPI algorithm after LBP algorithm implemented in the tomogram	153
5.26	Continue for LBPI technique	154
5.27	FBC using AGC technique for offline processing	155
5.28	Continue for FBC using AGC technique	156
5.29	Continue for FBC using AGC technique	157
5.30	Continue for FBC using AGC technique	158
6.1	Static experiment using six different object size	161
6.2	Two object flow in repeatability experiments	162

6.3	Gravity Flow Rig: (a) The actual flow rig (b) After installation with optical tomography system (c) The optical tomography system	165
6.4	Plastic beads	166
6.5	Three different baffle size	166
6.6	Three different location of baffle	167
6.7	Voltage Loss vs. Obstacle Diameter	168
6.8	Repeatability for all projection technique using LBP	170
6.9	AE_E (%) value for three types of single model using LBP algorithm via experimental works	178
6.10	AE_E (%) value for three types of single model using FBP algorithm via experimental works	179
6.11	PSNR for different projection and flow model using LBP, LBPI and FBP	180
6.12	NMSE for different projection and flow model using LBP, LBPI and FBP	180
6.13	Comparison of PSNR value between modeling and experiment for PB projection using single object	181
6.14	Comparison of PSNR value between modeling and experiment for MPFBC projection using single object	182
6.15	Comparison of PSNR value between modeling and experiment for MPFBLR projection using single object	182
6.16	Comparison of NMSE value between modeling and experiment for PB projection using single object	183
6.17	Comparison of NMSE value between modeling and experiment for MPFBC projection using single object	183
6.18	Comparison of NMSE value between modeling and experiment for MPFBLR projection using single object	184
6.19	AE_E (%) for various multiple flow models using FBP via experimental work	196
6.20	PSNR value for various multiple flow models using LBP via experimental work	197
6.21	NMSE value for various multiple flow models using LBP via experimental work	197

6.22	PSNR value for various multiple flow models using LBPI via experimental work	198
6.23	NMSE value for various multiple flow models using LBPI via experimental work	198
6.24	PSNR value for various multiple flow models using FBP via experimental work	199
6.25	NMSE value for various multiple flow models using LBPI via experimental work	199
6.26	Comparison of PSNR value between modeling and experiment for PB projection	200
6.27	Comparison of PSNR value between modeling and experiment for MPFBC projection	201
6.28	Comparison of PSNR value between modeling and experiment for MPFBLR projection	201
6.29	Comparison of NMSE value between modeling and experiment for PB projection	202
6.30	Comparison of NMSE value between modeling and experiment for MPFBC projection	202
6.31	Comparison of NMSE value between modeling and experiment for MPFBLR projection	203
6.32	The flow effect when arriving at the sensor location: (a) 10% baffle opening (b) 40% and 70% baffle opening	209
6.33	Comparison between calibration and measured mass flow rate for various baffle opening	213

LIST OF ABBREVIATIONS

LBP	-	Linear Back Projection
PSNR	-	Peak Signal to Noise Ratio
NMSE	-	Normalize Mean Square Error
ADC	-	Analogue to Digital Converter
I2C	-	Inter Integrated Circuit
FBP	-	Filtered Back Projection
PIC	-	Peripheral Interface Controller
AGC	-	Averaging Grouping Color
ECT	-	Electrical Capacitance Tomography
EIT	-	Electrical Impedance Tomography
PET	-	Positron Emission Tomography
SIE	-	Space Image Evaluating
NIR	-	Near Infrared
DSBP	-	Dynamic Sensitivity Back Projection
HRA	-	Hybrid Reconstruction Algorithm
GBP	-	Graphical Back projection
FBPR	-	Filtered Back Projection with 1/r Function
CBPR	-	Convolution Back Projection Ramp
CBPS	-	Convolution Back Projection Sinc
LS	-	Least Square
VB	-	Visual Basic
FBC	-	Fan Beam Centre
FBLR	-	Fan Beam Left and Right
MPFBC	-	Mix Projection between Parallel and Fan Beam Centre
MPFBLR	-	Mix Projection between Parallel and Fan Beam Left and Right

LBPI	-	Linear Back Projection with Interpolation
PB	-	Parallel Beam
AE	-	Area Error
SPFM16	-	Single Pixel Flow Model (16x16)
SPFM32	-	Single Pixel Flow Model (32x32)
FFM	-	Full Flow Model
PCB	-	Printed Circuit Board
SMD	-	Surface Mount Device
GUI	-	Graphical User Interface
GaAs	-	Gallium Arsenide
SR	-	Slew Rate
USART	-	Universal Synchronous Asynchronous Receiver Transmitter
FIFO	-	First In First Out
API	-	Application Programming Interface
MSE	-	Mean Square Error
SNR	-	Signal to Noise Ratio
RMSE	-	Root Mean Square Error
DAQ	-	Data Acquisition

LIST OF SYMBOLS

I	–	Output intensity (dimensionless)
I_0	–	Input Intensity (dimensionless)
μ	–	Attenuation Coefficient
$V_{max,}$	–	Maximum Voltage (V)
$V_{drop,}$	–	Voltage drop (V)
d	–	Particle Size (mm)
dB	–	decibel
As	–	Solid area percentage
A_G	–	Gas area percentage
$S_{Tx,Rx}$	–	Voltage value from each receiver
$\overline{MA}_{Tx,Rx}(x, y)$	–	Normalized sensitivity maps for each pair of transducer in the measured area of $x \times y$ matrix
$V_{LBP\_PB}(x, y)$	=	Voltage distribution obtained using LBP algorithm
A_M	–	Area from simulation modeling (mm^2)
A_A	–	Area from actual object (mm^2)
$f(x,y)$	–	Original Image
$f'(x,y)$	–	Reconstructed Image
n	-	Number of pixel
MAX	–	maximum possible pixel value
R_f	–	Feedback resistor (Ω)
I_{in}	–	Current input (A)
C_f	–	Feedback capacitor (Farad)
C_{in}	–	Input capacitance (Farad)

R_{in}	–	Input resistance (Ω)
bps	–	bit per second

Greek letters

μ	-	Attenuation Coefficient

LIST OF APPENDICES

APPENDIX	TITLE	PAGE
A	List of Publications	228
B	List of all tomogram result using LBP and FBP via simulation	236
C	List of all tomogram result using LBP and FBP via experiment	244
D	Source code for Master communication	252
E	Source code for Slave communication	257
F	Source code for VB programming	265

CHAPTER 1

INTRODUCTION

The word tomography is derived from the Greek word which means a slice of image. Technically, tomography is about obtaining cross sectional two or three dimensional images of *N*-dimensional object (Ai, 1996). Tomography has been adopted in many areas of the physical sciences and engineering to measure the distributions ("images") of parameters of interest in various processes (York *et al.*, 2011). Nowadays, tomography has been practiced on numerous applications in both medical and industrial field, whereby in industrial, the term for tomography is called process tomography.

It all began in the mid-1980s, where process tomography start to take place in the imaging system (A. Plaskowski *et al.,* 1995). The use of tomography would be beneficial especially in industrial applications that involve multiphase flow i.e., fluid-fluid flow, fluid gas flow, water oil flow and solid gas flow. Process tomography allows many kinds of parameter measurement such as velocity of the material, concentration profile, mass flow rate and the sizing of particles. All these parameters can be used in optimizing the design of the process flow. Through tomography measurement technique, the flow measurement can be continuously monitored without interrupting the flow object inside pipeline, and this may improve the inspection process in the industry. Many industries still perform common method in monitoring the pipeline flow, for example in palm oil industry where the palm oil

will be segregate into useful oil content and wasted sludge content. The sludge content will undergo the oil processing procedures again in the pipeline to identify remaining palm oil. By applying the tomography technique, we can identify the percentage of useful oil and sludge waste in the pipeline. By this, we could reduce the processing time and unnecessary oil refinery process.

In solid gas industry, there is a need to monitor and determine blockage in the pipeline and to verify whether the measurement subjects are flowing as required (Global Spec, 2011). Another important issue is to monitor the loss in the production for example in rice industry. From the industrial visit to Faiza factory, the monitoring system is important to monitor the weight of the rice before and after the enhancement process of rice quality. The current system applied in this factory make the production become slower and therefore they stop using the system. By applying mass flow rate meter using optical tomography approach, the rice weighing process will consume shorter time. In addition, current existing system used in the industry could only provide measurement readings and unable to identify the material distribution and movement in the pipeline. (Dickin *et. al.,* 1992) in the pipeline. Tomography system has the ability to visualize the tomogram image inside the pipeline. Therefore, problems such as blockages or unexpected processing results which may affect or change the flow of the solids and reduce the effectiveness can be solved easily with the help of this system.

In tomography system, set of sensors are arranged and mounted on the periphery of the pipeline to observe material flow characteristics inside the pipe. This advantage will reduce the cost of operation and may help the company to increase its profit and reduce losses.

1.1 Background Research Problem

Since the introduction of process tomography in industrial area, research in tomography has been rapidly applied. Solid subjects are one of the materials that often used in the industry. Solid is tend to distribute in non homogeneous way and that its velocity is not uniform (Arakaki *et. al.*, 2006). This is a major problem while measuring a two phase flow (Zheng and Liu, 2010) as it may affect the mass flow rate measurement which varies with time while transporting the material. Therefore, online mass flow rate is required to monitor for any changes in the pipeline. The system should also be able to identify any changes in real time and provide information whether the transportation of materials has a problem or not. Besides that, a study from Yingna Zheng *et. al.* (2010), has found that although two decades have passed, no online mass flow rate that is capable of giving an absolute measurement has been successfully built. Online mass flow rate plays an important role to measure the amount of materials being transported without having to weigh it using traditional way which is time consuming and need human resource monitoring.

According to the above, we now know the important of mass flow rate measurement which is really needed to help the current industrial process flow. Another issue in this field, the mass flow rate involves heavy computation when using inferential method. Inferential method is an indirect technique in getting the mass flow rate data, where it involves values from concentration profile and velocity profile (Beck, 1987). This will affect the real time component which is really crucial in mass flow rate. This issue can be solved by using a direct method and it will be applied in this project. Direct method involves a sensing element that produces the result of mass flow rate directly through the sensing components. Using this technique, the computation problem can be solved because the direct technique is free from any complex mathematical formula.

Other than that, image blurring and ambiguous are also major problems that should be addressed in optical tomography when using Linear Back Projection (LBP)

algorithm (Lei *et. al*., 2009) where the image quality are often affected. Image quality can be analyzed using certain parameters such as Peak Signal to Noise Ratio (PSNR) and Normalize Mean Square Error (NMSE). The higher the PSNR and the lower the NMSE value show an excellent quality of image. LBP is the main algorithm in this project. By using a single type of projection, which is parallel beam projection, the image quality will be quite poor. Therefore to solve this problem, some modifications have been done by combining it with a fan beam projection. These modifications improve the image quality.

1.2 Problem Statements

In optical tomography, several fields of studies are needed to accomplish the overall task.

- The sensor unit must be properly selected to make sure that the overall performance of the system is at its best condition. This is because, sometimes the sensors in the market does not fit with each other and produces unwanted noise to the circuit. The selection must also fulfill the required angle for parallel and fan beam projection and it also must have a fast switching time to enable both combination of projection to be implemented in the system and produce the image needed in real time.

- The signal conditioning and control unit are also the critical part in this project. This is because the amounts of sensors are quiet high, therefore, the Analogue to Digital (ADC) conversion would require much longer time to process.

- The image reconstruction technique using LBP algorithm was used because it is faster for image reconstruction technique in real time application. However, at the same time, the produced image has a smearing effect and the

quality which is not very good. Other algorithms such as Linear Back Projection with Interpolation (LBPI) and Filtered Back Projection (FBP) using Averaging Grouping Color (AGC) have been used as a post processing technique to enhance the image quality.

- The measurement of mass flow rate using gravity conveyer can be done by exploiting the values of concentration profile and velocity profile. However, this technique involves heavy computations. Therefore, the direct technique of measuring mass flow rate is selected to make sure it can measure the mass flow rate quickly.

1.3 Aim and Objectives of the Study

1.3.1 Aim

The aim of this research is to enhance the image quality using the mix projection between parallel and fan beam.

1.3.2 Specific Objectives

This research was carried out according to the following objectives.

i. To design the tomographic measurement hardware
ii. To design the tomographic software display
iii. To integrate the hardware and software for verification purpose

1.4 Scopes of the Study

i) The object that will be tested is assumed to have the same characteristics with the assumption that the attenuation factor is one for solid and the attenuation factor for air is zero. Therefore, all of the lights are assumed be absorbed by the object that neglecting the reflection, refraction and other nonlinearity effects of the light

ii) This research is concentrating on solving the problem that happens in parallel beam mode by combining parallel and fan beam projection.

iii) The mass flow rate experiment is only focusing on one material which is plastic beads.

iv) This research will use LBP as its main algorithm and focus on enhancement after the image has been acquired via offline technique.

1.5 Significant Research Contribution

The ability to implement a fan beam projection in parallel view is one of the novelties in this research. This design involves a sensor jig designed specifically for parallel applications that does not involve collimator design. Therefore the fan beam can also be implemented in the same sensor jig without difficulty.

The method to overcome the disadvantages of parallel beam projection seems to be a very practical solution to the problems that arise in a parallel beam. Although fan beam has its own disadvantages, combining these two approaches is expected to further enhance the image quality and can be measured using PSNR and NMSE parameters. The combination also eliminates the unwanted noise that appear when using parallel beam projection.

The mass flow rate measurement can be done in single plane by exploiting the concentration profile values which using the polynomial equation. This technique can eliminate the complex calculations between concentration and velocity profile.

1.6 Organization of the Thesis

This thesis is divided into 7 chapters. Chapter 1 presents the overview of the research project. It starts with the introduction of tomography in general and next covers the background of research problems and then explains the problem statement. The aim and objectives will give clearer information on the target of this study. Lastly, significance of the research and its contribution are discussed.

Chapter 2 presents the latest and crucial literature survey of this research. Therefore, any new research by the other researchers can be compared.

Chapter 3 is mainly about system modeling in optical tomography. The characteristics of light can be predicted to ensure the methodology used is suitable with that characteristic. This chapter also explains the mode of projection used in this research and lastly it explains the mass flow rate measurement and the calibration involve before the real measurement take place.

Chapter 4 is about image reconstruction algorithm that mainly focuses on Linear Back Projection (LBP). LBP is used for online system. Other algorithm such as LBPI and FBP with AGC method will be implemented via offline mode. The entire algorithm will be tested in three different projections where the purpose is to evaluate whether the combination projection between parallel and fan beam can enhance the tomogram image performance.

Chapter 5 explains the methodology used in hardware and software development. The hardware development includes the subtopics of sensor selection for emitter and receiver, circuit explanations, signal conditioning and data acquisition technique. For software development, it explains the overall program structure for every projection and algorithm.

Chapter 6 further discusses the research results and analysis where it gives the results from the experiment that include static and dynamic experiment.

Chapter 7 provides details on future works on how to improvise this research and gives suggestions for forthcoming upgrades.

CHAPTER 2

LITERATURE REVIEW

2.1 Introduction

There are various tomography types and optical tomography is chosen in this research. Optical tomography started to be focused starting from 1996 and right now its development is still gotten in curiosity by researchers. To develop an effective optical tomography system, the selection of transmitter and receivers should be focused carefully. This is the first step of the development of system and any failure in this stage; affect the whole process in the development of optical tomography. Along this selection, researchers also must have the idea on how they want to set up the projection because it is important in the sensor selection. After the successful in the sensor system, it's time to concentrate on the image reconstruction where the right choosing of the algorithm is vital. Lastly, is the parameter of interest in optical tomography; concentration profile and mass flow rate where the literature is focusing on mass flow rate as it always gets in attention by the researcher in this area.

2.2 Introduction to Process Tomography

Tomography flow measurement is well known in the industrial process. Tomography is vital to investigate activities of internal structures of a vessel without the need to invade it. There are several important parameters that can be investigated using tomography method such as mass flow rate, velocity profile and concentration profile. These parameters are crucial for industrial processes as these parameters help in monitoring the process control effectively and obtains good quality product with high safety features. Several methods of tomography are being used in industrial applications and one of it is optical tomography introduced by Abdul Rahim (1996). Optical tomography can be applied whether in industrial or medical application. Figure 2.1 shows the overall process of an optical tomography system.

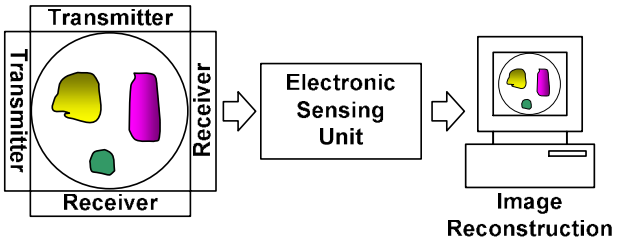

Figure 2.1: Optical tomography system

2.3 Types of Tomography Sensors

2.3.1 Electrical Capacitance Tomography (ECT)

ECT is a "soft field" tomography type and is widely used in applications that involve dielectric materials. Previous research shows that it can successfully be applied for two or more component flow such as solid/gas (Wang, *et al.*, 2010), oil/gas/water (Ismail, *et al*., (2005), water/steam (Jaworek *et al*., 2004) and gas/liquid/solid (Warsito and Fan, 2003). ECT had been used in many industrial applications, such as imaging of gas-oil flows in oil pipelines, gas-solids distribution in pneumatic conveyors and fluidized beds, combustion flame in engine cylinders and liquid droplets distribution in wet gas separators (ECT Instrument Limited, 2009). ECT has a non-linear relationship between electrical measurements and the permittivity of the measured material which makes the image reconstruction for ECT complicated. ECT is also unable to give high definition image boundaries and the sensitivity for the measured properties is not constant within the region of interest compared to computed tomography based on radiation or optical sensor (Green *et al*., 1997). However, ECT has some advantages such as there is no radiation, rapid response, low cost, better temporal resolution, non-intrusive and non-invasive, and able to withstand high temperature and high pressure. ECT works by calculating the changes in capacitance from a multi-electrode sensor. This is due to the change in permittivity of materials being visualized.

2.3.2 Electrical Impedance Tomography (EIT)

The primary aim of an EIT is to measure the distribution of electrically conductive components and it will reconstruct the impedance distribution parameter in the process and it is developed for clinical purpose in early 1980s (Plaskowski,

1995) where the application was subsequently extended to process control. The basic methodology for both applications is that it will illustrate the distribution of conductivity or permittivity within a volume whether it is a part of a human body or content of a pipeline (Denai *et al*., 2010). Current will be injected and voltage will be measured in EIT. The point electrode that is positioned around the vessel will make electrical contact with the fluid inside the vessel. Therefore, the material for the electrode must be more conductive than the material in the vessel.

The advantages of EIT are low cost technique, simple application, provides high speed of data collection and able to characterize the materials (Brown, 2001). There were three major areas that have always been a hot topic with this technology which are physical construction of the hardware, the use of multi-frequency data capture and three dimensional EIT. However, one main disadvantage of this technique is that EIT cannot be used for pneumatic conveying which contains large electrically non-conducting solids (Chan, 2002).

2.3.3 Ultrasonic Tomography

The basic principle of ultrasonic tomography is that the object or field will interact with an ultrasonic beam via acoustic scattering. To get the information about the objects/field, the interaction must be sensed. There are different ways to generate ultrasound such as using magnetostrictive, laser or capacitive techniques and piezoelectric material (Hauptmann *et al*., 1998). Ultrasonic uses non-invasive and non-intrusive technique. This type of tomography has the potential for imaging component flows such as oil/gas/water mixtures that occur in oil industry (Zhong, *et al*., 2005). Ultrasonic tomography also can be applied in transportation to evaluate the concrete pavements (Hoegh *et al.,* 2011).

The advantages of ultrasonic sensors is that the technique is non invasive, provides in-line measurement, rapid response, low power consumption, excellent long term stability and high resolution and accuracy. However, ultrasound is unsuitable for solid gas application because the speed of sound in gas limits the data acquisition rate (Syed Salim, 2003) and will produce high level of noise at the transducer because of the particle impact. Therefore, this technique is unsuitable for solid gas material.

2.3.4 Positron Emission Tomography (PET)

Positron emission tomography (PET) is a nuclear medical imaging technique for quantitative measurement of physiologic parameters in vivo, based on the detection of small amounts of positron-emitter-labeled biologic molecules. PET also can be applied in flow measurement where it is useful for imaging in opaque fluids, opaque pressure boundaries, and multiphase studies (Ruggles *et al.,*2011).

The advantage of this method is able to identify the positions of individual particles in the medium and not bulk masses as in X-ray tomography. However the disadvantage is corresponding to a safety problem for the patient where the radioactive isotope is required to be injected into the body and this limits its applications to laboratory studies or processes.

2.3.5 X-Ray Tomography

X-ray computed tomography has excellent spatial resolution but poor temporal resolution (Heindel *et al*., 2008). Spatial resolution is the measurement of

how closely lines can be resolved in an image. Temporal resolution is the precision of measurement with respect to time where the longer the light has to travel, the lower the temporal resolution is.

X-ray tomography provides a more quantitative imaging modality than others used for multiphase flow measurement such as electrical impedance and capacitance tomography. High speed gamma ray tomography using multiple fan beam collimated radioisotope source is a sufficient and fast method to visualize the cross sectional imaging in dynamic flow for different industrial process (Maad and Johansen, 2008).

2.3.6 Optical Tomography

The general principle of optical tomography is a set of light sources and the photo detectors are used into obtaining the parallel views of the pipeline. This type of tomography is popular for medical and process tomography. Recent research conducted is focusing more on the medical side rather than the process. Optical tomography is a "hard field" type tomography where it is sensitive to the parameters that they measure in all positions of measurement volume and it is very easy to obtain the data because the sensitivity is equal in all positions. It is, however, the opposite with "soft field" where the parameter sensitivity is dependent on the position of the sensors in the measurement volume. In optical, a beam of light will be projected through some medium from one boundary point and this light will be detected at another boundary point. At the receiving point, the level of voltage will be measured and any reduction of the value, is proportional to the existing object in the pipe or vessel. It means the optical tomography detects the attenuation of the signal.

The advantages of optical tomography are;

a) the response time is negligible due to the speed of light,
b) a very high resolution can be obtained from a small wavelength,
c) measurements are immune to electrical noise or interference,
d) wide selection of readily available emitters and detectors and
e) better spatial resolution.

Although it can be regarded as the simplest type of tomography, it also has its drawback. Light can travel to non-opaque objects. Therefore, non-opaque objects cannot be used, as it will not be able to give any reading to the receiving end. In addition, the opaque object is the most suitable material to be tested, but problem will occur, when two objects overlap each other, as it will be hard to distinguish them. This can be solved by using many projections and also by combining the parallel and the fan beam. This is the angle to be focused in this research.

2.4 Recent Research in Optical Tomography

There are many research works and groups that had established their own research niche in optical tomography. Sheffield Hallam University, for example is among the active groups involved in optical tomography. Their research focuses on a variety of experiments which utilize optical sensors (Dugdale *et al*., 1992; Abdul Rahim, 1996; Ibrahim, 2000). The ongoing research in Universiti Teknologi Malaysia (UTM) focuses on solid gas where some of them used parallel and fan beam projection. The most frequent sensors used in their research are infrared LED, laser and fiber optic (Chan, 2002; Pang, J.F., 2004; Goh, C.L., 2005; Mohamad, 2005; Abdul Rahim *et al*., 2008; Rasif, 2009; Abdul Rahim *et al*., 2009). Other related groups are from Zheijiang University, China, which focused on near infrared laser and Terahertz PT (Process Tomography) (Chen *et al*., 2005; Zhang *et a*l., 2005). Ozanyan *et al.* (2011) also made some effort in Terahertz filed. The group from Guangdong University of Technology, China studied the fan beam optical

sensor and its application in mass flow rate measurement of pneumatically conveyed solids (Li *et al*., 2005; Zheng *et al*., 2006). In Beijing Institute of Petrochemical Technology, Yan *et al*. (2005) worked on the optical tomography using optical fiber with an addition of artificial intelligent elements in their design. A researcher from Technical University of Opole, Poland used optical tomography in different types of research. The research is concerned with the implementation of optical tomography in a water tank (Rzasa and Plaskowski, 2003) and dual tomography, which was proven to improve the image reconstruction (Rzasa, 2009).

2.5 Overview of Transmitter and Receiver used in Optical Tomography

2.5.1 Transmitter

Lighting signal produced by a transmitter is crucial in optical tomography system. The transmitter that is suitable for optical tomography is Light Emitting Diode (LED), fiber optic and laser.

Light Emitting diode or LED has a long-lifetime and its light output exhibit a gradual reduction over the period of time. LED can be divided into 3 main colour which are red, yellow and green. Comparing the three LEDs, the Red LEDs seems to be more robust then the other two while the green one failed after several months without knowing the reason. LED can be classify into two categories which is visible LED and infrared (IR) LED. There are different electrical characteristic for both two where IR LED is usually has a lower forward voltage than visible LED (Held, 2009). However for visible LED, excessive current and low reverse voltage could destroy the LED (Soar, 1981).

Besides LED, fiber optic also is one of the sources of transmitter and its characteristic is promising. Fiber optic has a low power, high sensitivity, wide bandwidth and known to its resistance to electromagnetic interference Their price also has dropped and it surely will attract more users to utilize the device.

For laser as a source of transmitter, the laser diode is the device that has been selected to be discussed here. Both LED and laser diode are fabricated on similar semiconductor material but it operated differently where laser produce coherent light whereas LEDs do not. The bandwidth and the cost for laser diode is higher compared to LED. Thoughe LED have a more longevity characteristic compared to laser diode (Held, 2009).

2.5.2 Receiver

At the receiver side, it consists of several parts and among of it is photodetector, amplifier and filter. Photodetector will convert the received optical signal into a photocurrent which is photon to electron converter. Two types of photodetector that is widely used are p-i-n photodiode and avalanche photodiode. The different between them is how the electron-hole pair will be generated. For p-i-n photodiode, every time the photon is absorbed by the detector, the electron-hole pair will be generated. For avalanche photodiode, the electronic gain within the detector will generate that matter (Richard and Byron, 2002).

Other type of photodetector that is used by researchers is phototransistor. Although it has higher sensitivity, the response is slow and it is not suitable for tomography as tomography involve a dynamic flow. Phototransistor is designed to pick up sufficient quantities of light, thus makes it have unsatisfactory high-frequency response.

2.6 The Selection of Optical Sensor and Projection Arrangement: Advantages and Disadvantages

The selection of the optical sensors is crucial in the first stage of tomography. To ascertain that the system will operate efficiently, a comprehensive selection of the sensors must be performed. The selection of the sensors is influenced by the projection arrangement of the selected optical sensors. These are parallel beam mode and fan beam mode.

For parallel beam mode, the sensors have a narrow angle beam while fan beam mode uses wide angle beam. Both projections; parallel and fan beam mode have their own advantages and disadvantages. The main difference between parallel beam and fan beam modes is depicted in Figure 2.2.

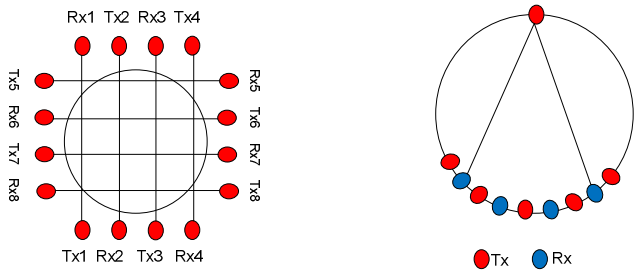

(a) (b)

Figure 2.2: a) Parallel beam projection, b) fan beam projection

In parallel beam projection, the sensor is arranged as one transmitter to one receiver. Meanwhile, for fan beam mode, one transmitter covers several receivers. As shown in Figure 2.2(a), the parallel beam projection is simple and easy to implement. This is because all transmitters and receivers will be 'ON' at the same time and no switching control is needed on the transmitter part. However, this simple construction has poor coverage where the line of light is straight and only certain parts will be covered. Blank spots or parts that cannot be detected will directly affect the tomogram result.

For fan beam mode as shown in Figure 2.2 (b), the detection coverage is 100% of the pipe cross section. However, the vital drawback of this mode is that the switching process of the detectors from one transmitter to another transmitter until the entire transmitter array finished performing the scanning, critically delays the detection period. Investigations were carried out to identify the best detection for optical tomography by coupling different sensor methods to different beam modes. The investigated groups are listed as below:

a) fiber optic and parallel beam mode, (Abdul Rahim, 1996;Ibrahim, 2000)

b) LED and fan beam mode (Chan, 2002; Zeng, 2001),

c) infrared and parallel beam mode (Pang, 2004; Goh, 2005; Chiam, 2006; Dugdale, 1992),

d) infrared and fan beam mode (Leong, 2005),

e) laser and parallel beam mode (Mohamad, 2005; Mohamad *et. al.,*2006),

f) laser and fan beam mode (Chen *et. al*., 2005; Zheng *et. al*. 2006) and

g) dual mode (Rasif, 2009; Rzasa, 2009).

2.6.1 Fiber Optic and Parallel Mode

The preparation of fiber optics in optical tomography was a challenging job as incorrect cutting procedures will cause fault measurement. Therefore, careful setup of the system is necessary. Abdul Rahim, (1996) and Ibrahim, (2000) have reported on optical tomography using fiber optics for measuring different materials.

Abdul Rahim (1996) used fiber optic as a sensor tool. The diameter of pipe in his research was 81mm. The light source was a single quartz halogen that provided a large beam area. It produced good illumination for all the optical transmitter fibers, which were arranged in a bundle. The receiver fiber converted the signals into electrical signals by PIN diodes. Although only 16 pairs of fiber optic transmitters and receivers were used and arranged in two projections, it is still

capable in producing the concentration profile and tomographic images successfully. Besides that, this research also performs well in getting the result for particle size distribution. The assumption used to obtain the results is to ignore the effect of scattering and diffraction of light (Abdul Rahim, 1996). One drawback of fiber optics is that the transmitters and receivers need to be aligned accurately. Otherwise, the sensors will produce incorrect readings and this can greatly reduce the accuracy of the system. Another problem arises would be related to the light collimating issue where the arrangement of transmitters and receivers in a group might create a problem since the possibility of overlapping is higher between adjacent receivers. This results in intensity loss. Although there are negative effects, fiber optics provide the opportunity to design sensors with a wider signal bandwidth which enables measurements of higher speed flowing particles. Some improvements in image reconstruction algorithm are need to obtain a better image as well. Apart from that, the CPU speed and data acquisition need to be improved to make the system more reliable.

Ibrahim, (2000) has put in some enhancements in optical tomography. The fiber optics used in his experiment were arranged in two planes, which was different from Abdul Rahim, (1996) who used only one plane. Each plane consists of two rectilinear and two orthogonal projections. For orthogonal, 8 by 8 sensors were implemented while for rectilinear, 11 x 11 sensors were used. The total numbers of transmitter sensors in one plane were 38. The unique feature was the implementation of four 35cm projectors as light source and light guide. This research ignores the scattering effects and also neglects the fibre cladding as it is assumed thin in comparison to the central fibre. As a result, small bubbles in diameter of 1-10 mm and volumetric flow rate up to 1 l/min can be detected using optical tomography. The optical tomography is sensitive to large bubbles in water of diameter 15-20 mm and volumetric flow rates up to 3 l/min (Ibrahim, 2000). This modification produces a result with higher resolution than the previous research done by Abdul Rahim, (1996) due to the increment in the number of sensors. However, the arrangement of the receivers and transmitters in a group will result in overlapping beam for the

receivers. Different forms of filtering techniques in reconstruction algorithm should also be investigated in order to produce better results.

2.6.2 LED and Fan Beam Mode

The best characteristics about LED are the minimal power drawn, its longevity and its cost compared to many other sensors (Chen *et. al*., 2011). LED has slow rise time and fall time, but it can still be used in optical tomography system as was demonstrated by Chan, (2002) and Zeng *et al*., (2001). They proved that LED is feasible for optical tomography applications.

Chan, (2002) used LED as a source of light and PIN photodiode as a receiver, both with diameters of 2.94 mm. The sensors were arranged in a fan beam projection technique and the total number of sensors installed are 16 pairs as shown in Figure 2.3. The fan beam method exploits a larger emission angle of the source that was feasible to be sent to all the receivers and the emission power is uniform along the projection. There are a few assumptions that had been made which include:

i) Light scattering and beam divergence effect are neglected.

ii) The attenuation factor for air is assumed to be zero while the attenuation factor for solid particle is assumed to be one. All incident lights on the solid surface are fully absorbed.

iii) Single projection resulted in 16 light beams from the emitter towards the photodiodes and each of the light beams possesses a different width, depending on the sensor geometry and projection angle.

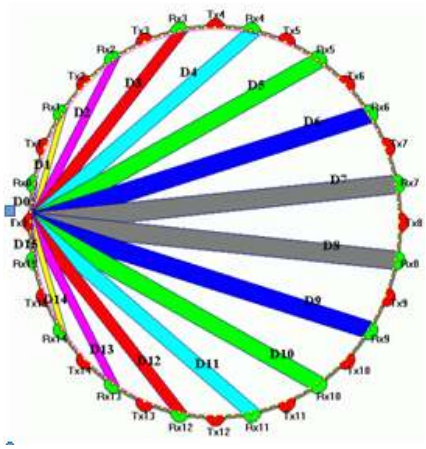

Figure 2.3: Sensor arrangement used 16 pairs of sensor

Zeng *et. al*. (2001) chose red LED as the source of a transmitter and in parallel with the light that will be detected by photo valve at the other side. They used rotary working table for the experiment setup to get the complete projection for the object. In this project, they employed one of the optical scattering methods, which is light extinction method but ignored the diffraction effect that is formed by the edged of the particles. Sand in a diameter of 120 μm was dropped through a funnel and the flow velocity was observed to be dependent on the controlled funnel. Thus, by changing the velocity, different optical signal would be obtained. From the experiment, random fluctuation signal was produced, where it was related with the light decrement. As the light decreased, more particles were shown to be passing through, that blocked the light source which is an indication of a higher mass concentration.

2.6.3 Infrared Led and Parallel Beam Mode

Infrared LED has a characteristic of invisible to human eyes, and it is more difficult to handle compared to LED as it was hard to check for alignment. However, this type of sensing element is recommended since its wavelength is outside of visible light; therefore, the interruption of day light can be avoided. Pang, (2004),

Goh, (2005) and Chiam, (2006) are among the researchers that used infrared in parallel projection for optical tomography.

Pang, (2004) used infrared LED from TEMIC Semiconductor model TSUS4300 that had a wavelength in the range of 900 to 1000 nm, whereas the peak of wavelength was at 950 nm. Thus, the optical tomography sensor designed is indisputably unaffected by the visible light source from the surrounding environment that will result in error during the measurement process. The features of a small angle of half intensity, which was 16° is a main criteria to take into account because they implement parallel beam mode in their project. For the receiver, Pang, (2004) had chosen phototransistor instead of photodiode due to compatibility of phototransistor model, TEFT4300 to the infrared LED. The advantage of phototransistor was that the starting wavelength of phototransistor was about 875nm that was well away from the visible light's boundary, 700nm. Most photodiode available in the market are sensitive to visible light. It has a physical size of 3 mm in diameter, peak of wavelength is 925 nm, and angle of half sensitivity was 30 degree and less costly.

For the experiment purposes, Pang, (2004) used plastic pellets, which look like a small cylinder in dimension of 2 x 2 x 3 mm to be imaged. It will be tested to observe the difference of concentration profile in four kinds of a regime (full flow, three quarter flow, half flow and quarter flow). To measure the mass flow rate, three other regimes were set up with a diameter of 4.5 cm, 4 cm and 3.5 cm. The dropping distance is 16 cm and 56 cm. The smaller the drop distance, it will produce higher concentration (Abdul Rahim *et al.,* 2005b).

For the projection technique, Pang, (2004) implemented two orthogonal and two rectilinear projections per layer (16 pairs for one orthogonal projection and 23 pairs for one rectilinear projection) as shown in Figure 2.4.

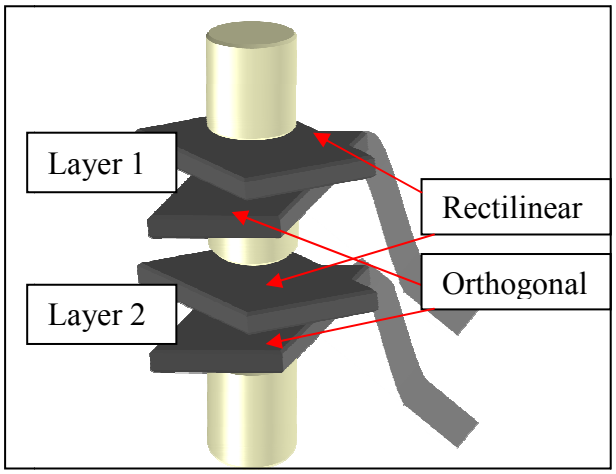

Figure 2.4: Two layer of projection by Pang, (2004)

This projection method has doubled the amount that Ibrahim, (2000) did and this has enhanced the resolution. The two plane arrangement (upstream and downstream) may cause misalignment of objects that passed through from an upper stream to downstream because they cannot be projected in the same layer. This will affect the velocity parameter in this system. Therefore, the distance between two orthogonal and two rectilinear needs to be reduced where the better solution is to make all the projection in the same layer. Nevertheless, this type of projection can successfully determine the online mass flow rate without involving any calibration constant. There is still some improvements that can be done in this research to improve the time to get the mass flow rate measurement and the tomogram image. It is suggested to use a higher sampling rate of DAS card rather than DAS-1802HC. Another alternative is to design simple and cheaper data acquisition system using, for example, Ethernet, USB, DSP and FPGA technologies. Furthermore, the computational issue in this project should be addressed, where; it involved four powerful personal computers and a network hub in order to implement a data distribution system. This would result in a large and non-portable system.

Goh, (2005) identified Pang's problem and applied single plane for the system as shown in Figure 2.5. It has improving the system because all

REFERENCES

Abdul Rahim, R. (1996). A tomography imaging system for pneumatic conveyors using optical fibres. Doctor Philosophy. Sheffield Hallam University.

Abdul Rahim, R. and Green, R.G. (1998). Optical Fibre Sensor for Process Tomography. *Control Engineering Practice*. 6(11), 1365-1371.

Abdul Rahim, R. Rahiman, M.H.F., Goh, C.L., Muji, S.Z.M. and Yunos, Y.M. (2010). Modeling orthogonal and rectilinear mixed-modality projection of optical tomography for solid-particles concentration measurement. Sensors and Actuators A: Physical, 161(1-2), 53-61.

Abdul Rahim, R., Chan, K.S., Pang, J.F. and Leong, L.C. (2005a). A hardware development for optical tomography system using switch mode fan beam projection. *Sensors and Actuators A: Physical*. 120(1), 277-290.

Abdul Rahim, R., Chiam, K.T., Pusppanathan, J. and Susiapan, Y.S.-L. (2009). Embedded system based optical tomography: the concentration profile. *Sensor Review*. 29(1), 54-62.

Abdul Rahim, R., Leong, L.C., Chan, K.S. Rahiman, M.H. and Pang, J.F. (2008). Real time mass flow rate measurement using multiple fan beam optical tomography. *ISA Transaction* 47(1), 3-14.

Abdul Rahim, R., Pang, J.F. and Chan, K.S. (2005b). Optical tomography sensor configuration using two orthogonal and two rectilinear projection arrays. *Flow Measurement and Instrumentation.* 16(5), 327-340.

Acharya, T. and Tsai, P.S. (2007). Computational Foundations of Image Interpolation Algorithms. *ACM Digital Library.* 8(42).

Ai, M. (1996). Future of Imaging Technology. *Sensors and Actuators A: Physical*. 56(1-2), 31-38.

Arakaki, C., Ratnayake, C. and Halstensen, M. (2010). Online prediction of mass flow rate of solids in dilute phase pneumatic conveying systems using multivariate calibration. *Powder Technology*. 195, 113–118.

Barnett, R.H., O'Cull, L. and Cox, S.A. (2004). *Embedded C Programming and the Microchip PIC*. New York: Thomson Delmar Learning.

Barrat, I.R., Yan, Y., Byrne, B. and Bradley, M.S.A. (2000). Mass flow measurement of pneumatically conveyed solids using radiometric sensors. *Flow Measurement and Instrumentation*. 11(3), 223-235.

Beck, M.S., Green, R.G. and Thorn, R. (1987). Non-intrusive measurement of solids mass flow in pneumatic conveying. *Journal of Physics E: Scienctific Instruments.* 20(7), 835-840.

Birtalan, D. and Nunley, W. (2009). *The Photodiode. Infrared-Visable-Ultraviolet Devices and Applications*. (2nd ed.). Boca Raton F.L.: CRC Press.

Brown, B.H. (2001). Medical impedance tomography and process impedance tomography: a brief review. *Measurement Science and Technology*. 12(8), 991-996 .

Burr Brown Corporation. (1994). *Desingning Photodiode Amplifier Circuit with OPA128.* Retrived 13 November 2010 from http://focus.ti.com.lit/an/sboa061.pdf**.**

Carter, R.M. and Yan, Y. (2005). An instrumentation system using combined sensing strategies for online mass flow rate measurement and particle sizing. *IEEE Transactions on Instrumentation and Measurement*, 54(4), 1433-1437.

Censor, Y. (1983). Finite Series - Expansion Reconstruction Methods. *Proceedings of the IEEE.* 71(3), 409-419.

Chan, K.S. (2002). *Real Time Image Reconstruction For Fan Beam Optical Tomography System.* Master Engineering. Universiti Teknologi Malaysia.

Chen, A., Yang, Y., Alqasemi, U., Aguirre, A. and Zhu, Q. (2011). A low cost multi-wavelength tomography system based on LED sources. *Progress in Biomedical Optics and Imaging - Proceedings of SPIE*. 7896.

Chen, J., Hou, D., Zhang, T. and Zhou, Z. (2005). Near infrared laser computed tomography test-system design and application. *Flow Measurement and Instrumentation.* 16(5), 321-325

Chiam, K.T. (2006). Embedded System based Solid-Gas Mass Flow rate Meter using Optical Tomography. Master Engineering. Universiti Teknologi Malaysia.

Denai, M.A., Mahfouf, M., Mohamad-Samuri S., Panoutsos, G**.,** Brown, B.H. and Mills, G.H. (2010). Absolute electrical impedance tomography (aEIT) guided ventilation therapy in critical care patients: Simulations and future trends. *IEEE Transactions on Information Technology in Biomedicine*, 14(3), 641-649.

Dickin, F.J., Hoyle, B.S., Hunt, A., Huang, S.M., Ilyas, O., Lenn, C., Waterfall, R.C., Williams, R.A., Xie, C.G. and Beck, M.S. (1992). Tomographic imaging of industrial process equipment: techniques and applications. *IEEE Proceeding on Circuits, Devices and Systems*. 139(1), 72-82.

Dugdale, P., Green, R.G., Hartley, A.J., Jackson, R.G. and Landauro, J. (1992). Optical Sensors for Process Tomography. *ECAPT*. Manchester, 26-29

Dyakowski, T. (1995). Tomography in a process system. In Williams, R.A and Beck, M.S. (1st ed.) *Process Tomography: Principles, Techniques and Applications* (pp. 13-36). London: Butterworth-Heinemann Ltd.

ECT Instrument Limited (2009). Electrical Capacitance Tomography. Retrieved 19 Disember 2009, from http://www.ect-instruments.com/ect.htm**.**

Gajewski, J. B. (2008). Electrostatic Nonintrusive Method for Measuring the Electric Charge, Mass Flow Rate, and Velocity of Particulates in the Two-Phase Gas Solid Pipe Flows: Its Only or as Many as 50 Years of Historical Evolution. *IEEE Transactions on Industry Applications.* 44(5), 1418-1430.

Garner, W. (2007). *Area of an Ellipse.* Retrived 12 September 2011 from http://math.ucsd.edu/~wgarner/math10b/area_ellipse.htm.

Global Spec. (2011). *Solids Flow Meters.* Retrived 29 November 2011 from http://www.globalspec.com/learnmore/sensors_transducers_detectors/flow_sensing/flommeters_solids.

Goh, C.L. (2005). Real-Time Solids Mass Flow Rate Measurement Via Ethernet Based Optical Tomography System. Master Engineering. Universiti Teknologi Malaysia

Green, R.G., Rahmat, M.F., Evans, K., Goude, A., Henry, M. and Stone, J.A.R. (1997). Concentration profiles of dry powders in a gravity conveyor using an electrodynamics tomography system. *Measurement Science and Technology*. 8, 192-197.

Hauptmann, P., Lucklum, R., Püttmer, A. and Henning, B. (1998). Ultrasonic sensors for process monitoring and chemical analysis: state-of-the-art and trends. *Sensors and Actuators A: Physical*. 67(1-3), 32-48.

Heindel, T.J., Gray, J.N. and Jensen, T.C. (2008). An X-ray system for visualizing fluid flows. *Flow Measurement and Instrumentation.* 19(2), 67-78.

Held, G. (2009). *Introduction to Light Emitting Diode Technology and Applications*. CRC Press Taylor and Francis Group, United State.

Herman, G.T. (1995). Image Reconstruction From Projection. *Real Time Imaging.* 1(1), 3-18.

Hoegh, K., Khazanovich, L. and Yu, H. T. (2011). Ultrasonic tomography for evaluation of concrete pavements. *Transportation Research Record, National Research Council*. 2232, 85-94.

Ibrahim, S. (2000). Measurement of Gas Bubbles in a Vertical Water Column using Optical Tomography. Doctor Philosophy. Sheffield Hallam University.

Ismail, I., Gamio, J.C., Bukhari, S.F.A. and Yang, W.Q. (2005). Tomography for multi-phase flow measurement in the oil industry. *Flow Measurement and Instrumentation.* 16(2-3), 145-155.

Jackson, R.G. (1995). The Development of Optical Systems for Process Imaging. In Williams, R.A and Beck, M.S. (1st ed.) *Process Tomography: Principles, Techniques and Applications* (167-179). London: Butterworth- Heinemann Ltd.

Jaworek, A., Krupa, A. and Trela, M. (2004). Capacitance sensor for void fraction measurement in water/steam flows. *Flow Measurement and Instrumentation.* 15(5-6), 317-324.

Jerald, G.G. (1996). *Photodiode Amplifier - Op Amp Solutions*. New York: McGraw-Hill.

Kak, A.C. and Slaney, M. (1988). *Principles of Computerized Tomographic Imaging*. (1st ed.). New York: IEEE Press.

Kole, J.S. (2005). Statistical image reconstruction for transmission tomography using relaxed ordered subset algorithms. *Physics in Medicine and Biology.* 50(7), 1533-1545.

Kugelstadt, T. (2003). Active Filter Design Techniques. In Mancini, R. *Op Amps for Everyone*. (26-324). New York: Elsevier Newnes.

Lei, J., Liu, S., Li, Z.H., Meng, S. (2009). An image reconstruction algorithm based on the extended Tikhonov regularization method for electrical capacitance tomography. *Measurement.* 42 (3), 368-376.

Leong, L.C. (2005). Implementation of multiple fan beam projection technique in optical fibre process process tomography. Master Engineering. Universiti Teknologi Malaysia, Skudai.

Lewitt, R.M. (1983). Reconstruction Algorithms: Transform Method. *Proceeding of the IEEE.* 71(3), 390-408.

Li, Y., Zheng, Y.-N. and Yue, H.-W. (2005). Design of fan beam optical sensor and its application in mass flow rate measurement of pneumatically conveyed solids. *Zhejiang University SCIENCE A.* 6A (12), 1430-1434.

Liu, S., Chen, Q., Wang, H.G., Jiang, F., Ismail, I. and Yang, W.Q. (2005). Electrical capacitance tomography for gas-solids flow measurement for circulating fluidized beds. *Flow Measurement and Instrumentation.* 16(2-3), 135-144.

Maad, R. and Johansen, G.A. (2008). Experimental analysis of high-speed gamma ray tomography. *Measurement Science and Technology.* 19(8), 1-10 .

Macal, C.M. (2005). Model Verification and Validation. *Workshop on Threat Anticipation: Social Science Methods and Models.* University of Chicago.

Mancini, R. (2003). Single-supply Op Amp Design Techniques. In Mancini, R. *Op Amps for Everyone*. (29-50). New York: Elsevier Newnes.

Matworks (2011). Product Documentation: The Inverse Radon Transformation. Natick, Massachusetts, U.S.A.

Mchugh, S. (2011). *Digital Image Interpolation.* Retrived, 31 December 2011 from http://www.cambridgeincolour.com/tutorials/image-interpolation.htm.

Mohamad, E.J. (2005). *Flame Imaging using Laser Based Transmission Tomography*. Master Engineering. Universiti Teknologi Malaysia.

Mohamad, E.J. Rahim, R. A., Ibrahim, S., Shahrum, S., Manaf, M.S. (2006). Flame imaging using laser-based transmission tomography. *Sensors and Actuators A: Physical.* 127(2), 332-339.

Muji, S.Z.M., Abdul Rahim, R. and Rahiman, M.H. (2010). Sensitivity Map in Parallel and Fan Beam mode in Optical Tomography. *6th World Congress on Industrial Process Tomography (WCIPT6).* Beijing, China, 762-771.

Muji, S.Z.M., Abdul Rahim, R., Rahiman, M.H.F, Abdul Shaib, M.F., Sahlan, S., Muhammad Jaysuman and Mohamad, E.J. (2011). Optical Tomography: A Review on Sensor Array, Projection Arrangemnet and Image Reconstruction Algorithm. *International Journal of Innovative Computing, Information and Control.* 7(7A), 3839-3856.

Nor Ayob, N. M. (2011). Development of Ultrasonic Tomography System for Liquid/Gas Flow Measurement in a Vertical Column. Master Engineering. Universiti Malaysia Perlis.

Ozanyan, K.B., Wright, P., Stringer, M.R. and Miles, R.E. (2011). Hard-Field THz Tomography. *IEEE Sensors Journal.* 11(10), 2507 – 2513.

Pang, J.F. (2004). *Real-Time Velocity and Mass Flow Rate Measurement using Optical Tomography*. Master Engineering. Universiti Teknologi Malaysia, Skudai.

Pease, B. (2001). *What's All This Transimpedance Amplifier Stuff, Anyhow? (Part 1)* Retrived 17 Jun 2009 from http://electronicdesign.com/article/analog-and-mixed-signal/what-s-all-this-transimpedance-amplifier-stuff-any.aspx.

PerkinElmer Optoelectronics (2010). *Characteristics of Phototransistors*. Retrived 20 Julai 2009 from http://optoelectronics.perkinelmer.com/content/ApplicationNotes/APP_PhototransistorCharacteristics.pdf

Plaskowski, A., Beck, M.S., Thorn, R. and Dyakowski, T. (1995). *Imaging Industrial Flows*. London: Institute of Physic Publishing Ltd.

Rahiman, M.H.F (2005). Non-Invasive Imaging of Liquid/Gas Flow using Ultrasonic Transmission-Mode Tomography. Master Engineering. Universiti Teknologi Malaysia.

Rahmat, M.F. and Tajdari, T. (2011). Particles Mass Flow Rate and Concentration Measurement using Electrostatic Sensor. *International Journal on Smart Sensing and Intelligent Systems.* 4(2), 313-324.

Rasif, M.Z. (2009). The Development of a Dual Modality Tomography (DMT) System using Optical and Capacitance Sensors for Solid/Gas Flow Measurement. Master Engineering. Universiti Teknologi Malaysia.

Smith R. G. and Kasper, B. L. (2002). Optical Receivers. In Gibson, J. D. *The Communication Handbook*. CRC Press.

Ruggles, A.E., Zhang, B.Y. and Peters, S.M. (2011). Positron Emission Tomography (PET) for Flow Measurement. *Advanced Materials Research.* 301-303, 1316-1321.

Rzasa, M.R. (2009). The measuring method for tests of horizontal two-phase gas-liquid flows, using optical and capacitance tomography. *Nuclear Engineering and Design.* 239(4), 699-707.

Rzasa, M.R. and Plaskowski, A. (2003). Application of optical tomography for measurements of aeration parameters in large water tanks. *Measurement Science and Technology.* 14(2), 199-204.

Schleicher, E., Da Silva, M.J., Thiele, S., Li, A. Wollrab, E. and Hampel, U. (2008). Design of an optical tomograph for the investigation of single- and two-phase pipe flows. Measurement Science and Technology, 19(9), 1-14.

Syed Salim, S.N. (2003). Concentration Profiles and Velocity Measurement using Ultrasonic Tomography. Master Engineering. Universiti Teknologi Malaysia.

Soar, R. N. (1981). *50 Simple L.E.D. Circuits*. (1st ed). Great Britian: Bernard Babani Publisher.

Song, D., Peng. L., Lu, G., Yang, S. and Yan, Y. (2009). Digital Image Processing based Mass flow Rate Measurement of Gas/Solid Two Phase Flow. *Journal of Physics.* 147, 1-8.

Vishay Semiconductor. (2005). *TSUS4300 Infrared Emitting Diode, 950 nm, GaAs*. Retrived 13 December 2009 from http://www.vishay.com/docs/81053/tsus4300.pdf**.**

Waltz, E. and Waltz, T. (2009). Principles and Practice of Image and Spatial Data Fusion.In Hall, D.L. and Llinas, J. *Handbook of Multisensor Data Fusion.* Florida : CRC Press.

Wang, F., Zhao, Y., Marashdeh, Q. and Fan, L.S. (2010). Horizontal gas and gas/solid jet penetration in a gas-solid fluidized. *Chemical Engineering Science.* 65(11), 3394-3408.

Warsito, W. and Fan, L.S. (2003). ECT imaging of three-phase fluidized bed based on three-phase capacitance model. *Chemical Engineering Science.* 58(3-6), 823-832.

Wikipedia. (2011). *Peak signal-to-noise ratio.* Retrived, 29 September 2009 from http://en.wikipedia.org/wiki/Peak_signal-to-noise_ratio.

Xie, C.G. (1995). Image Reconstruction. In Williams, R.A and Beck, M.S. (1st ed.) *Process Tomography: Principles, Techniques and Applications* (pp. 281-319). London: Butterworth-Heinemann Ltd.

Xie, C.G., Beck, M.S., Reinecke, N. Mewes, D. and Williams, R.A. (1995). Electrical tomography techniques for process engineering applications. *The Chemical Engineering Journal and the Biochemical Engineering Journal.* 56(3), 127-133.

Yan, C., Zhong, J., Liao, Y., Lai, S., Zhang, M. and Gao, D. (2005). Design of an applied optical fiber process tomography system. *Sensors and Actuators B: Chemical.* 104(2), 324-331.

Yan, Y. (1996). Mass flow measurement of bulk solids in pneumatic pipelines. *Measurement Science and Technology.* 7, 1687–1706.

Yan, Y., Xu, L. and Lee, P. (2006). Mass Flow Measurement of Fine Particles in a Pneumatic Suspension Using Electrostatic Sensing and Neural Network Techniques. *IEEE Transactions on Instrumentation and Measurement.* 55(6), 2330-2334.

York, T., McCann, H. and Ozanyan, K.B. (2011). Agile Sensing Sytems for Tomography. *IEEE Sensors Journal.* 11(12), 3086-3104.

Zeng, N., Lai, S. and Liao, Y. (2001). Optical tomography for two phase flow measurement. *Proceedings of SPIE - The International Society for Optical Engineering.*4448, 341-347

Zhang, G.-X, Chen, J. and Zhou, Z.-K. (2005). Terahertz PT technology for measurement of multiphase flow and its infrared simulation. *Journal of Zhejiang University SCIENCE.* 6A(12), 1435-1440.

Zhang, J., Ma, S., Zhang, Y. and Zhao, D. (2009). *Lecture Notes in Computer Science (including subseries Lecture Notes in Artificial Intelligence and Lecture Notes in Bioinformatics)* 5879 LNCS , 1174-1184

Zhang, Y., Gao, Y., Xu, Q. and Zhou, F. (2007). Development and Study of Image Reconstruction Algorithm for Electrical Capacitance Tomography. *IEEE Conference on Industrial Electronics and Applications (ICIEA).* 2113-2117.

Zheng, Y. and Liu, Q. (2010). Review of certain key issues in indirect measurements of the mass flow rate of solids in pneumatic conveying pipelines. *Measurement*. 43(6), 727-734.

Zheng, Y., Li, Y. and Liu, Q. (2007). Measurement of mass flow rate of particulate solids in gravity chute conveyor based on laser sensing array. *Optics & Laser Technology.* 39(2), 298-305.

Zheng, Y., Liu, Q., Li, Y. and Gindy, N. (2006). Investigation on concentration distribution and mass flow rate measurement for gravity chute conveyor by optical tomography system. *Measurement.* 39(7), 643-654.

Zhong, X.-F., Wu, Y.-X., Li, D.-H., Li, Q. and Wang, X.-G. (2005). Ultrasonic tomography and its applications in oilfield. *Journal of Zhejiang University: Science,* 6(12), 1420-1423.